Electronic Supplementary Material (ESI) for Catalysis Science & Technology.

Supplementary information

Reverse water-gas shift reaction over $Pt/MoO_x/TiO_2$: reverse Mars-van Krevelen mechanism via redox of supported MoO_x

Shinya Mine,[a] Taichi Yamaguchi,[a] Kah Wei Ting,[a] Zen Maeno,[a] S. M. A. Hakim Siddiki,[a]

Kazumasa Oshima,[b] Shigeo Satokawa,[b] Ken-ichi Shimizu,*[a,c] Takashi Toyao*[a,c]

[a] Institute for Catalysis, Hokkaido University, N-21, W-10, Sapporo 001-0021, Japan

[b] Department of Materials and Life Science, Faculty of Science and Technology, Seikei University, Musashino, Tokyo 180-8633, Japan

[c] Elements Strategy Initiative for Catalysts and Batteries, Kyoto University, Katsura, Kyoto 615-8520, Japan

*Corresponding authors

Ken-ichi Shimizu, Takashi Toyao

E-mail: kshimizu@cat.hokudai.ac.jp, toyao@cat.hokudai.ac.jp

Methods

Chemicals and Preparation of the Catalysts

Chemicals and materials were purchased from commercial suppliers and used without further purification. TiO_2 (P25, 50 m^2/g) having both anatase and rutile phases was obtained from Evonik (formerly Degussa). TiO_2 STR-100N (100 m^2/g) having rutile phase was obtained from Sakai Chemical Industry while TiO_2 ST-01 (188 m^2/g) with anatase phase was obtained from Ishihara Sangyo. The following sentences have been added. The carbon support and MoO_3 were commercially obtained from Kishida Chemical. Al_2O_3 was prepared by calcination of boehmite (Catapal B, Sasol) for 3 h at T = 900 °C. ZrO_2 (JRC-ZRO-2) was supplied by the Catalysis Society of Japan. HZSM-5 with SiO_2/Al_2O_3 ratio = 22 was purchased from TOSOH Co., Ltd. SiO_2 (CariACT Q-10) was purchased from Fuji Silysia Chemical Company Ltd. Nb_2O_5 was prepared by calcination of niobic acid ($Nb_2O_5 \cdot nH_2O$, HY-340) supplied from CBMM (Companhia Brasileira de Metalurgia e Mineração), at 500 °C for 3 h. CeO_2 was prepared by calcination (600 °C, 3 h, in air) of CeO_2 (Type A) obtained from Daiichi Kigenso Kagaku Kogyo Co., Ltd. An industrial $Cu/Zn/Al_2O_3$ catalyst (MDC-7; Cu = 34 wt%) was obtained from Clariant. Another industrial $Cu/Zn/Al_2O_3$ catalyst known as a copper-based low temperature water-gas shift catalyst (HiFUEL® W220; CuO = 52 wt%, ZnO = 30 wt%, Al_2O_3 =17 wt%) and an industrial $FeCrCuO_x$ catalyst known as an iron-chrome based high temperature water-gas shift catalyst (HiFUEL® W210; Fe_2O_3 = 82.7 wt%, Cr_2O_3 = 7 wt%, CuO = 5 wt%) were purchased from Alfa Aesar.

$Pt(3)/MoO_x(15)/TiO_2$ (3 wt% Pt, 15 wt% MoO_3 (10 wt% Mo)) was prepared by using the sequential impregnation method. First, MoO_3-loaded TiO_2 ($MoO_3(15)/TiO_2$) was prepared by using impregnation of TiO_2. In the process, a mixture of 1.4 g of TiO_2 and 0.74 g of $(NH_4)_6Mo_7O_{24} \cdot 4H_2O$ in a 500 mL glass vessel containing 100 mL of deionized water was stirred for 15 min with 200 rpm agitation at room temperature. The mixture was evaporated to dryness at 50 °C, dried at 110 °C for 12 h and calcinated in air at 500 °C for 3 h to give $MoO_3(15)/TiO_2$. The formed $MoO_3(15)/TiO_2$ was then added to an aqueous HNO_3 solution containing $Pt(NH_3)_2(NO_3)_2$. The mixture was evaporated to dryness at 50 °C and further dried in air at 110 °C for 12 h to give $PtO_2(3)/MoO_3(15)/TiO_2$ (Unreduced sample). The catalyst used in the hydrogenation process was prepared by reduction of $Pt(3)/MoO_3(15)/TiO_2$ in a quartz tube under a flow of H_2 (20 $cm^3\ min^{-1}$) at 300 °C for 0.5 h to give $Pt(3)/MoO_x(15)/TiO_2$. The $Pt/MoO_x/TiO_2$ catalysts having different Pt and MoO_3 contents were prepared in the same manner using different amounts of $MoO_3(15)/TiO_2$ and $Pt(NH_3)_2(NO_3)_2$.

Other supported catalysts were prepared in the manner described above by using $MoO_3(15)/TiO_2$ and other metal sources including aqueous solutions of NH_4ReO_4, $RuCl_3$, $IrCl_3 \cdot nH_2O$, $AgNO_3$, $Cu(NO_3)_2 \cdot 3H_2O$, $Ni(NO_3)_2 \cdot 6H_2O$, and $Co(NO_3)_2 \cdot 6H_2O$ and aqueous HNO_3 solutions of $Rh(NO_3)_3$ and $Pd(NH_3)_2(NO_3)_2$. For the preparation of $Pt(3)/MO_x(15)/TiO_2$ (M = V and W), NH_4VO_3 and $(NH_4)_{10}W_{12}O_{41} \cdot 5H_2O$ were independently used as respective precursors, and the procedure is the same manner as described above.

Catalysts Characterization

X-ray diffraction (XRD) measurements were carried out using Miniflex (Rigaku) with CuKα radiation. AUTOSORB 6AG (Yuasa Ionics Co.) was used for the N_2 adsorption measurements. Scanning transmission electron

microscopy (STEM) observations were performed using a JEM-ARM200F microscope equipped with a JED-2300 EDX spectrometer (JEOL). Samples were prepared by dropping an ethanol solution containing the catalyst on carbon-supported Cu grids. Temperature programmed reduction with H_2 (H_2-TPR) was performed by using BELCAT II (MicrotracBEL) with a cryo apparatus. A sample was mounted in a cell and then heated at a ramping rate of 10 °C min^{-1} under a flow of 5% H_2/Ar (20 cm^3 min^{-1}). The effluent gas was passed through a trap system that contains MS4A to remove the produced water and then through a thermal conductivity detector (TCD) to determine the consumed amount of H_2 in the process. Due to the experimental setup, separate experiments were carried out using temperature range of -100-50 °C and 100-900 °C. Temperature-programmed oxidation (TPO) measurement was performed with the BELCAT II. 40 mg of the spent catalyst was used for TPO experiment. The catalyst was pretreated at 150 °C for 30 min under a He atmosphere. The gas flow was switched to 50% O_2/He (40 cm^3 min^{-1}) and then the temperature was increased to 800 °C at 5 °C/min. During the reaction, the CO_2 generated through coke oxidation (m/e = 44) was measured by mass spectroscopy (Belmass, MicrotracBEL).

X-ray photoelectron spectroscopy (XPS) for Mo 3d was carried out on Shimadzu ESCA-3400HSE, equipped with a modified UHV chamber using Mg Kα (1253.6 eV) radiation. Binding energies were calibrated based on the O1s peak energy (532.0 eV). The reduced samples were measured after the H_2 reduction using an Ar-filled glove box that was directly connected to the XPS chamber in order to avoid exposure of the samples to air.

XPS for Pt 4f was carried out on a JEOL JPS-9010MC spectrometer using Mg Kα (1253.6 eV) radiation. Binding energies were calibrated based on the C1s peak energy (285.0 eV). The reduced samples were measured after the H_2 reduction using a transfer vessel in order to avoid exposure of the samples to air.

In situ IR experiments were recorded on a JASCO FT/IR-4600 equipped with with a Mercury-Cadmium-Telluride (MCT) detector and a quartz IR cell connected to a conventional flow system (100 mL min^{-1}). The sample was pressed into a 40 mg self-supporting wafer and mounted in the quartz IR cell with CaF_2 windows. Spectra were measured by accumulating 20 scans at a resolution of 4 cm^{-1}. The reference spectrum of the catalyst wafer in He taken at the measurement temperature was subtracted from each spectrum.

Mo K-edge, Pt L_3-edge, and Ti K-edge X-ray absorption spectroscopy (XAS) were performed in a transmission mode at the BL14B2 of SPring-8 at the Japan Synchrotron Radiation Research Institute (JASRI). A Si(311) double crystal monochromator was used for the Mo K-edge and Pt L_3-edge XAS measurements while a Si(111) double crystal monochromator was used for the Ti K-edge XAS measurements. For *operando* Mo K-edge XAS measurements, a high-sampling-rate TCD GC (490 Micro GC; Agilent Technologies Inc.) was used for the quantitative analysis of CO and CH_4. A mass spectrometer was also used to monitor the eluent gas. Samples (ca. 28 mg) in pellet forms (φ7 mm) were introduced into a cell equipped with Kapton film windows and gas lines connecting to the GC. Pretreatment of the samples involved heating under a flow of 10% H_2/He (220 cm^3 min^{-1}) at 300 °C. Subsequently, 10%CO_2/He, 40%H_2/He, and 10%CO_2+40%H_2/He (220 cm^3 min^{-1}) were introduced into the cell with intervals of He purge between gas introduction. *Operando* Pt L_3-edge and Ti K-edge XAS measurements were performed in a similar manner except amounts of the samples and gas flow rates in order to obtain good XAS spectra with the transmission measurements. Sample weight of ca. 31 mg and total

flow rate of 240 cm^3 min^{-1} was employed for the Pt L_3-edge measurements while sample weight of ca. 3 mg and total flow rate of 100 cm^3 min^{-1} was employed for the Ti K-edge measurements in order to employ similar space velocity for the catalytic reaction. Note that boron nitride (BN) was used to make a pellet sample for the Ti K-edge measurements. The obtained XAS spectra were analyzed using Athena and Artemis software ver. 0.9.25 included in the Demeter package. Fourier transformation of the k^3-weighted EXAFS was conducted over a k range 3.0-15.0 $Å^{-1}$. Curve-fitting EXAFS analysis was performed using Athena software ver. 0.9.25 included in the Demeter package.

Operando DRIFT measurements were carried out on a JASCO FT/IR-4600 spectrometer with a MCT detector and a diffuse reflectance cell (JASCO DR-600Ai). The outlet line was connected to a home-made gas cell and the effluent gas was monitored by another JASCO FT/IR-4600 spectrometer (with TGS detector). Approximately 40 mg of the sample was set in the cell and pretreated under a flow of 10% H_2/He (50 cm^3 min^{-1}) at 300 °C. After cooling to 250 °C under flowing He, 100% CO_2 (25 cm^3 min^{-1}) was introduced. A reference spectrum, recorded at 250 °C under a flow of pure He, was subtracted from each spectrum.

Catalytic reverse water gas shift reaction (RWGS) reactions

RWGS reactions were carried out in a fix bed continuous flow reactor under atmospheric pressure. A quartz tube that has wide center with inner diameter of 10 mm was used for catalysts screening shown in Table 1 and investigations on the effect of loading amount of Pt and Mo shown in Figure 4 while straight channel quartz tube with inner diameter of 4 mm was used for the other studies. The catalyst was pretreated under a H_2 flow (40 cm^3 min^{-1}) prior to each activity tests. Catalytic activity was measured in the temperature range of 200-300 ˚C under the following composition of feed gas: 10 vol.% CO_2, 40 vol.% H_2, 45 vol% He and 5 vol.% N_2 with a total flow rate of 100 cm^3 min^{-1}. He is added as a balance gas and N_2 is added as an internal standard. The gas flows were controlled by mass flow controllers. The effluent gas phase was allowed to pass through an ice-bath unit to remove the water vapor and then analyzed online using a gas chromatograph (Agilent 490 Micro GC) equipped with Molsieve 5Å and PoraPLOT Q columns and TCD detector.

Comparison of RWGS catalytic performance

Table S1. Reports on catalytic RWGS reactions ($T \leq 250$ °C).

Catalyst	H_2/CO_2	T (˚C)	P (bar)	CO_2 conv. (%)	CO selec. (%)	CO formation rate (mmol g_{cat}^{-1} min^{-1})	Reference
$Pt(2)/CeO_2$	1	225	1	13.7	99.0	0.07	1
$Cu(10)\text{-}C/ZnO(5)/SiO_2$	3	250	30	6.0	99.0	<0.05	2
Li(10)-Rh(5)/Zeolite	3	250	30	13.0	87.0	0.12	3
$Rh(0.4)/SiO_2$	3	250	10	2.5	84.6	<0.05	4
K_{80}-Pt(0.05)/zeolite L	1	250	1	1.0	100	0.19	5
$Ni(2.4)/SiO_2$	4	250	1	3.2	100	0.18	6
Cu(0.3)MgAl-LDH	4	250	1	4.5	100	0.14	7
$Au(1)/TiO_2$	4	250	1	11.5	100	0.13	8
$Pt(5)/TiO_2$	1	250	1	4.0	97.5	0.07	9
$NH_2MPA/Pt(5)/TiO_2$	14	250	1	8.4	95.1	0.06	10
$Pt(1)/CeO_2$	1	250	1	0.6	100	0.06	11
$In_2O_3\text{-}CeO_2$	1	250	1	<0.1	-	<0.05	12
$Pd(3)In/SiO_2$	1	250	1	<0.1	-	<0.05	13
$Pt(3)/MoO_x(15)/TiO_2$[a]	4	250	1	4.1	100	1.11	This study
$Pt(3)/MoO_x(15)/TiO_2$[b]	4	250	1	1.3	100	0.35	This study
$Pt(3)/MoO_x(15)/TiO_2$[c]	4	250	1	9.4	100	0.66	This study

[a] Initial activity using 15 mg of $Pt(3)/MoO_x(15)/TiO_2$ (from Figure 6). [b] After 600 h of the reaction time using 15 mg of $Pt(3)/MoO_x(15)/TiO_2$ (from Figure 6). [c] Initial activity using 60 mg of $Pt(3)/MoO_x(15)/TiO_2$.

Supplementary results

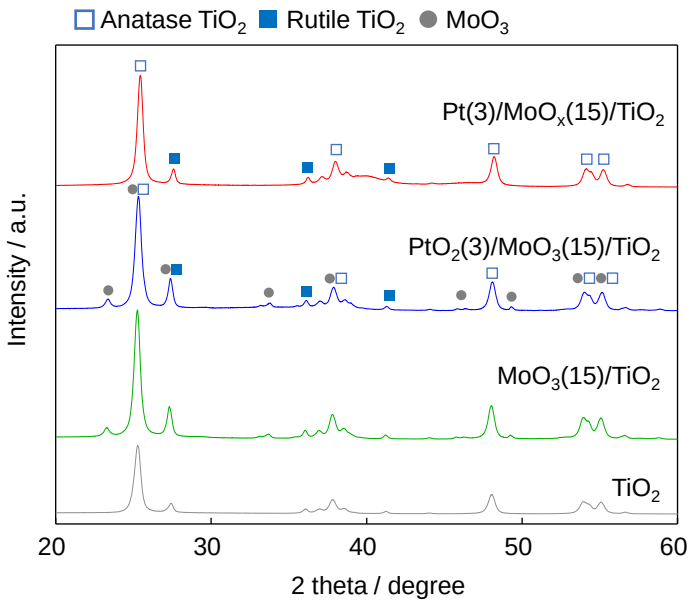

Figure S1. XRD patterns of pristine TiO_2, $MoO_3(15)/TiO_2$, $PtO_2(3)/MoO_3(15)/TiO_2$, and $Pt(3)/MoO_x(15)/TiO_2$.

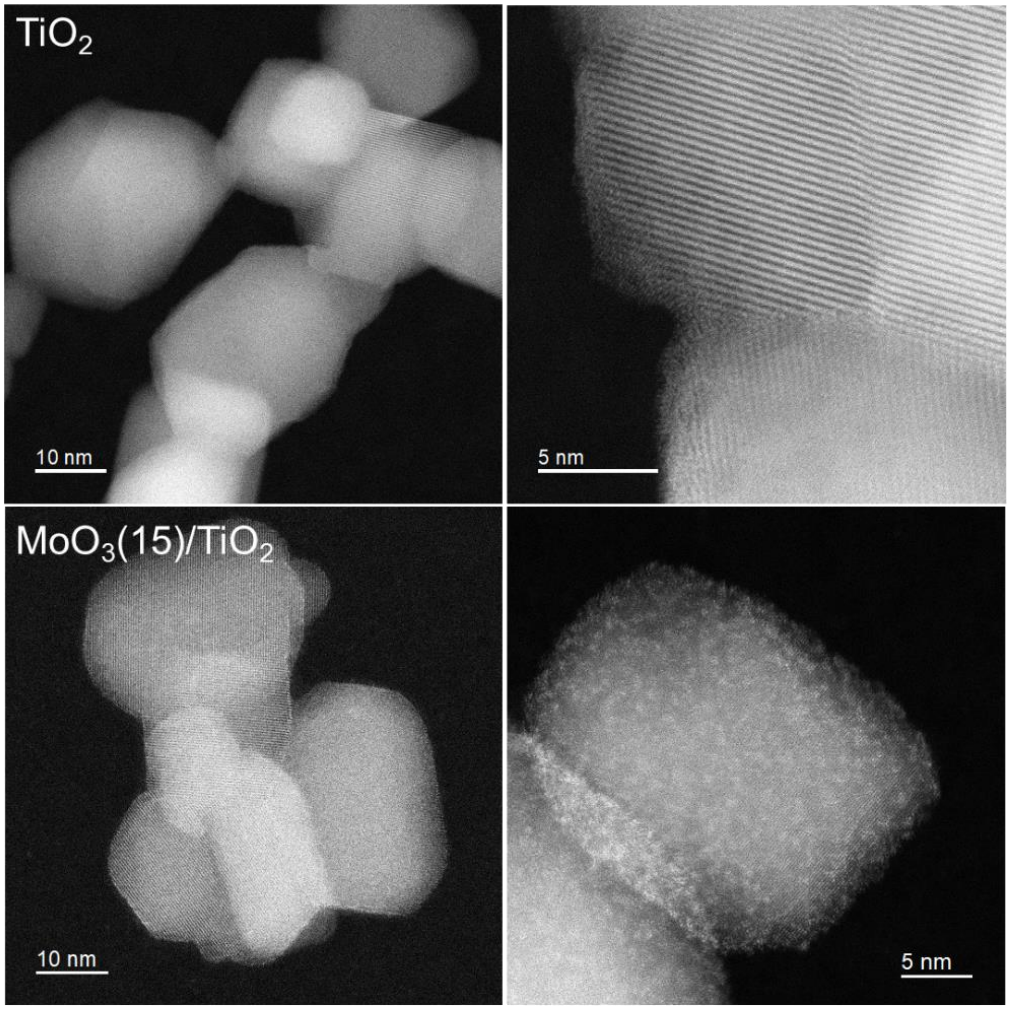

Figure S2. HAADF-STEM images for TiO_2 and $MoO_3(15)/TiO_2$.

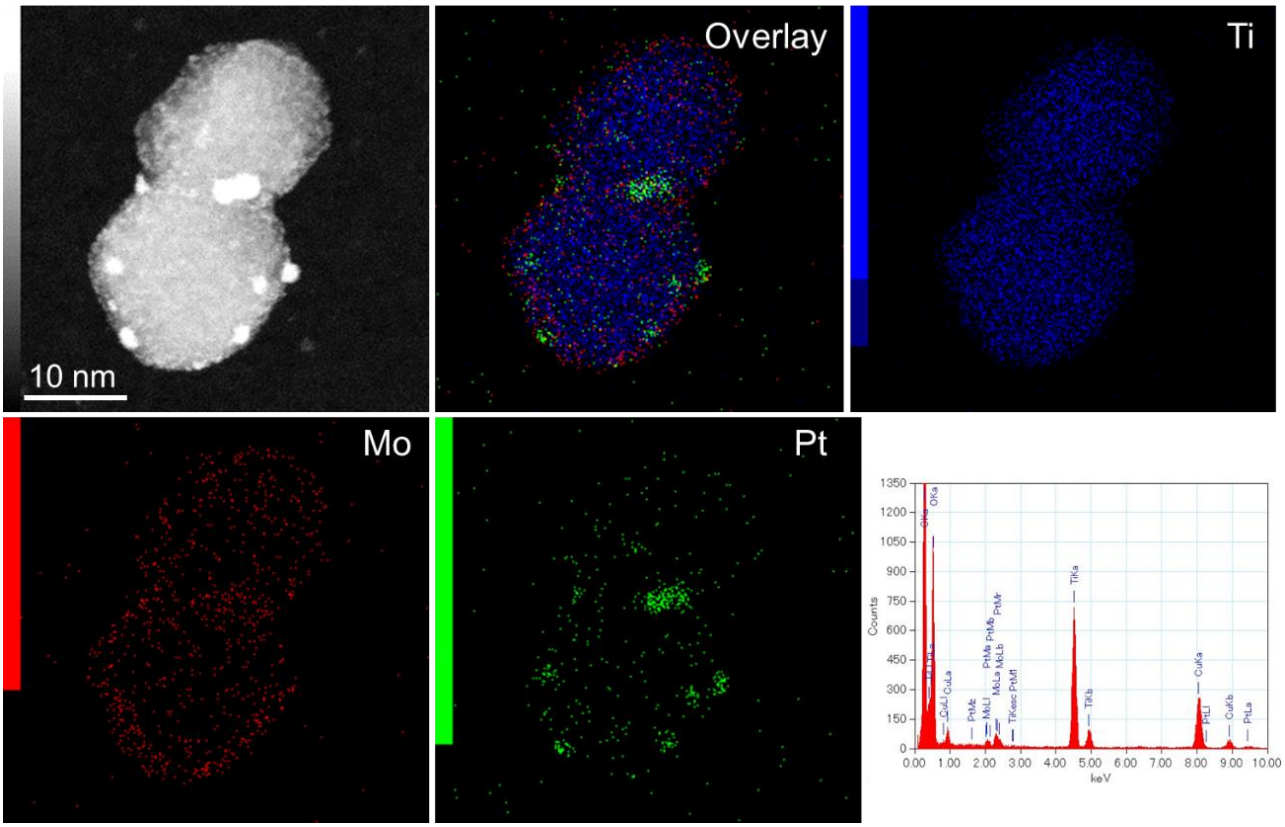

Figure S3. A HAADF-STEM image and EDX mapping for Pt(3)/MoO_x(15)/TiO_2. The Pt, Mo, Ti, and O signals are related to the catalyst composition. The C and Cu signals arise from the grid used for the measurement.

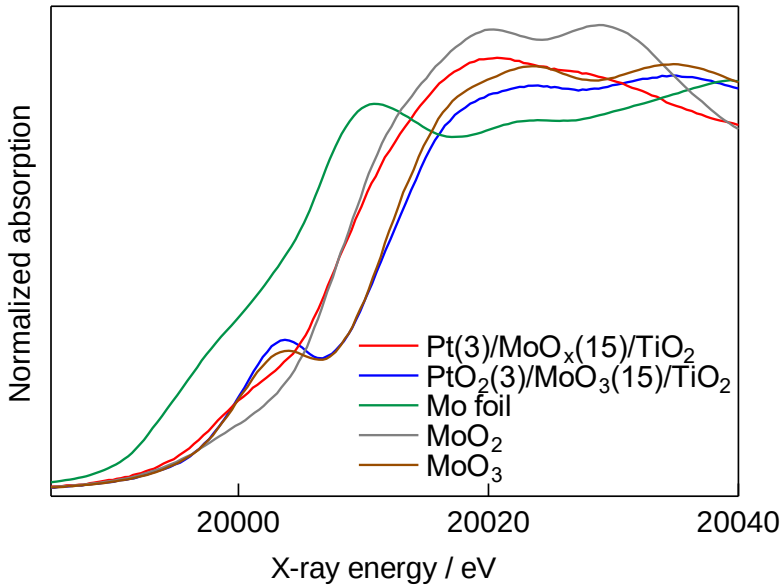

Figure S4. Mo K-edge XANES of PtO_2(3)/MoO_3(15)/TiO_2, Pt(3)/MoO_x(15)/TiO_2, and the reference compounds. A spectrum of Pt(3)/MoO_x(15)/TiO_2 was collected *in situ* at 300 °C just after the H_2 reduction at 300 °C. The other spectra were recorded at room temperature.

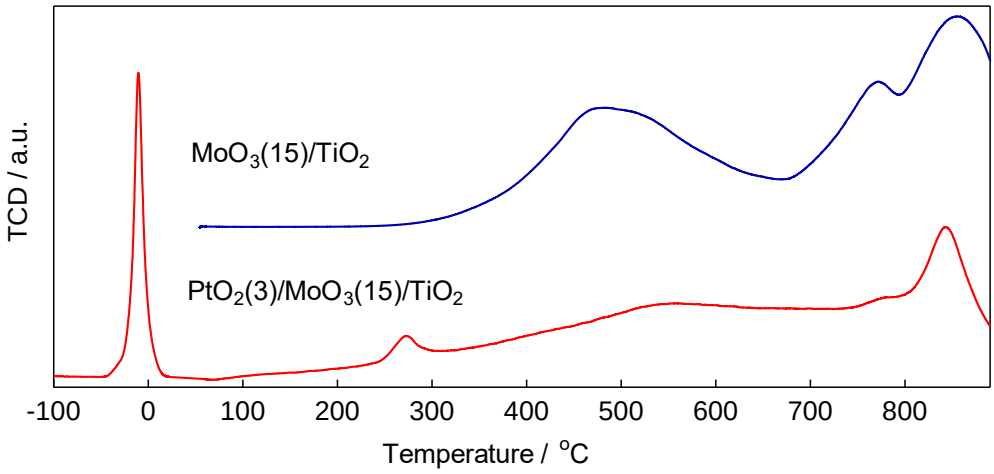

Figure S5. H_2-TPR profile of $MoO_3(15)/TiO_2$, and $Pt(3)/MoO_x(15)/TiO_2$. The sample was heated using a temperature ramp-rate of 10 °C min^{-1} in a flow of 5% H_2/Ar (20 cm^3 min^{-1}).

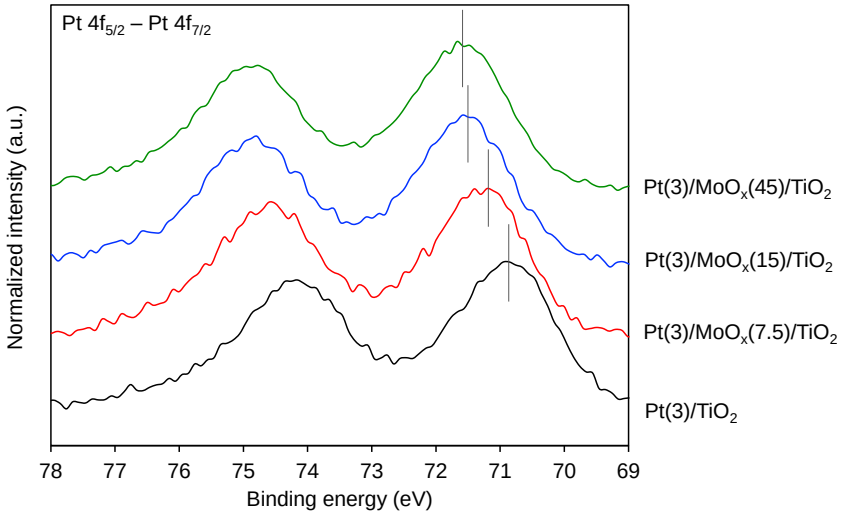

Figure S6. XPS spectra of the Pt 4f region of $Pt(3)/MoO_x/TiO_2$ (MoO_3 loading = 45, 15, and 7.5 wt%) and $Pt(3)/TiO_2$.

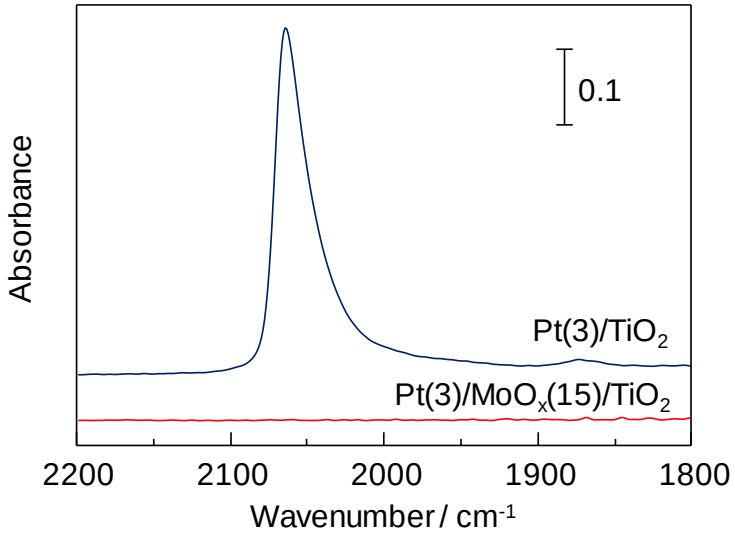

Figure S7. IR spectra of CO adsorbed on $Pt(3)/MoO_x(15)/TiO_2$ and $Pt(3)/TiO_2$ measured at 250 °C. After the H_2 reduction pretreatment at 300 °C, the sample was exposed to a flow of 1% CO/He (100 mL min^{-1}) for 5 min and purged with He for 5 min.

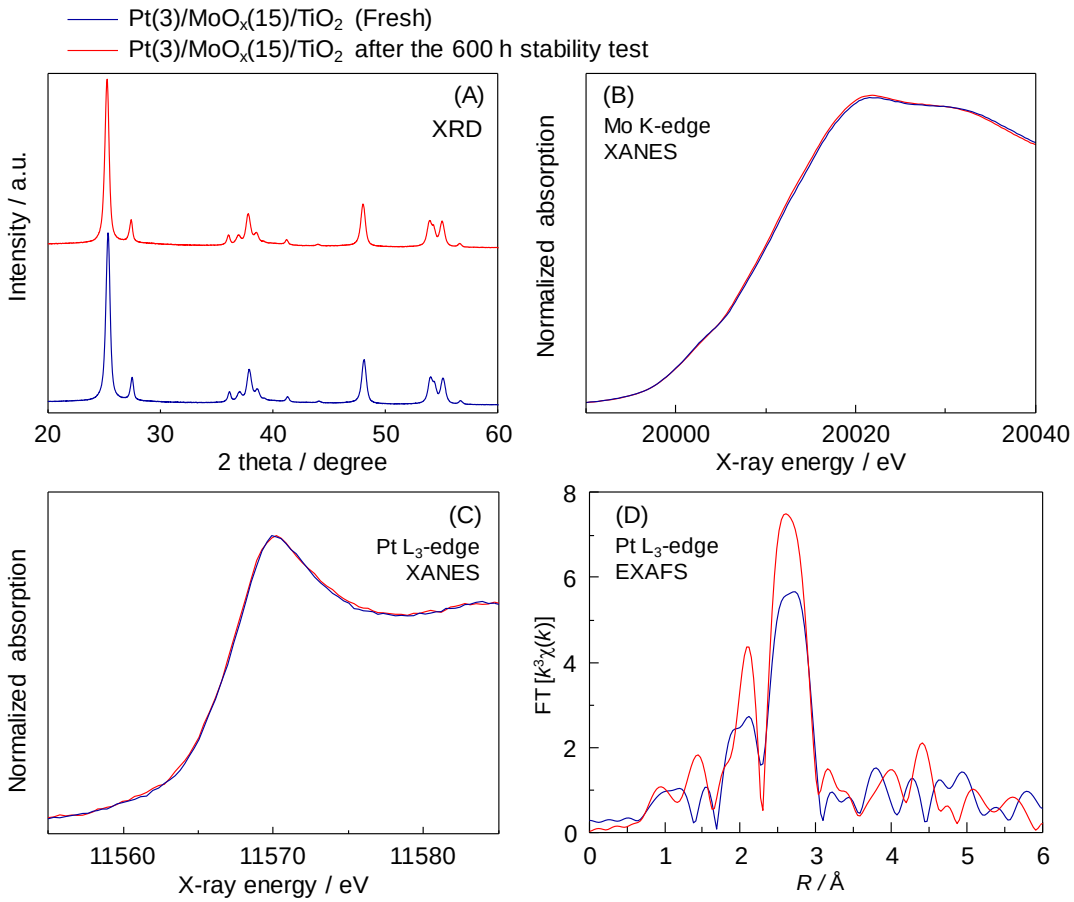

Figure S8. Structural analyses of Pt(3)/MoO_x(15)/TiO_2 before and after the long-term stability test (600 h RWGS reaction shown in Figure 6). (A) XRD patterns, (B) Mo K-edge XANES, and Pt L_3-edge (C) XANES and (D) FT-EXAFS. The XAS spectra were recorded at room temperature on samples that were not exposed to air after the reduction/reaction treatment and were contained in sealed vessels under N_2.

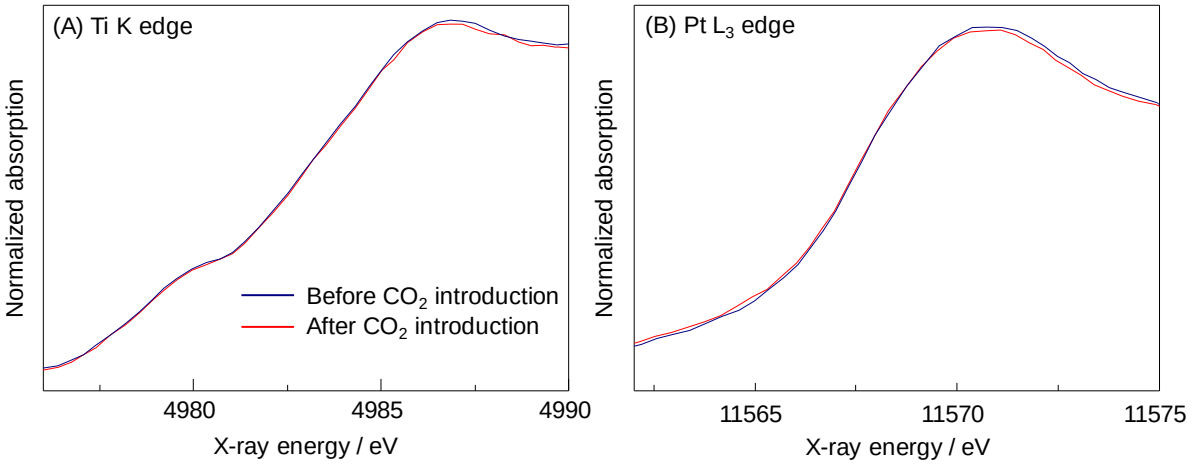

Figure S9. *Operando* (A) Ti K-edge and (B) Pt L_3-edge XANES of Pt(3)/MoO_x(15)/TiO_2 obtained at 250 °C after the H_2 reduction pretreatment at 300 °C (navy line) and after subsequent introduction of 10%CO_2/He (red line).

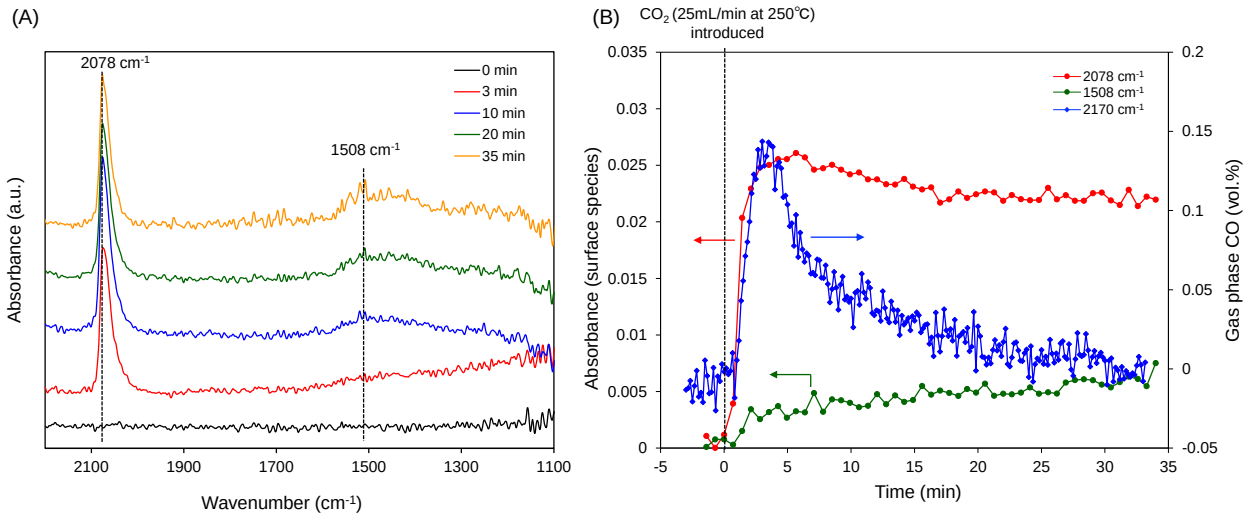

Figure S10. (A) *Operando* DRIFT spectra obtained at 250 °C after the H_2 reduction pretreatment and after subsequent introduction of 100% CO_2. (B) Variations in the intensities of peaks related to surface adsorbed species and the concentration of CO_2 in the effluent gas upon the introduction of 100% CO_2.

References

1 A. Goguet, F. C. Meunier, D. Tibiletti, J. P. Breen and R. Burch, *J. Phys. Chem. B*, 2004, **108**, 20240–20246.

2 X. Hu, X. Hu, Q. Guan and W. Li, *Sustain. Energy Fuels*, 2020, **4**, 2937–2949.

3 K. Kitamura, K. Soga, K. Kunimori and H. Arakawa, 1998, **175**, 67–81.

4 C. Wang, E. Guan, L. Wang, X. Chu, Z. Wu, J. Zhang, Z. Yang, Y. Jiang, L. Zhang, X. Meng, B. C. Gates and F. S. Xiao, *J. Am. Chem. Soc.*, 2019, **141**, 8482−8488.

5 X. Yang, X. Su, X. Chen, H. Duan, B. Liang, Q. Liu, X. Liu, Y. Ren, Y. Huang and T. Zhang, *Appl. Catal. B Environ.*, 2017, **216**, 95–105.

6 R. V. Gonçalves, L. L. R. Vono, R. Wojcieszak, C. S. B. Dias, H. Wender, E. Teixeira-Neto and L. M. Rossi, *Appl. Catal. B Environ.*, 2017, **209**, 240–246.

7 Y. Chen, H. Hong, J. Cai and Z. Li, *ChemCatChem*, 2021, **13**, 656−663.

8 L. F. Bobadilla, J. L. Santos, S. Ivanova, J. A. Odriozola and A. Urakawa, *ACS Catal.*, 2018, **8**, 7455−7467.

9 X. Chen, X. Su, H. Duan, B. Liang, Y. Huang and T. Zhang, *Catal. Today*, 2017, **281**, 312–318.

10 J. Zhang, S. Deo, M. J. Janik and J. Will Medlin, *J. Am. Chem. Soc.*, 2020, **142**, 5184–5193.

11 X. Chen, X. Su, B. Liang, X. Yang, X. Ren, H. Duan, Y. Huang and T. Zhang, *J. Energy Chem.*, 2016, **25**, 1051–1057.

12 W. Wang, Y. Zhang, Z. Wang, J. M. Yan, Q. Ge and C. J. Liu, *Catal. Today*, 2016, **259**, 402–408.

13 J. Ye, Q. Ge and C. J. Liu, *Chem. Eng. Sci.*, 2015, **135**, 193–201.